Boundary Slip on Smooth Hydrophobic Surfaces: Intrinsic Effects and Possible Artifacts

C. Cottin-Bizonne, B. Cross, A. Steinberger, and E. Charlaix*

Laboratoire de Physique de la Matière Condensée et Nanostructures, Université Claude Bernard, 6 rue Ampère, 69622 Villeurbanne CEDEX, France

(Received 6 September 2004; published 10 February 2005)

We report an accurate determination of the hydrodynamic boundary condition of simple liquids flowing on smooth hydrophobic surfaces using a dynamic surface force apparatus equipped with two independent subnanometer resolution sensors. The boundary slip observed is well defined and does not depend on the scale of investigation from one to several hundreds of nanometers, nor on shear rate up to $5 \times 10^3\ s^{-1}$. The slip length of 20 nm is in good agreement with theory and numerical simulations concerning smooth nonwetting surfaces. These results disagree with previous data in the literature reporting very high boundary slip on similar systems. We discuss possible origins of large slip length on smooth hydrophobic surfaces due to their contamination by hydrophobic particles.

DOI: 10.1103/PhysRevLett.94.056102 PACS numbers: 68.08.–p, 47.15.Gf, 68.15.+e

The growing interest for flows at small scales or in confined geometries has raised the need for a precise description of transport properties of liquids near a solid-liquid interface. If it is now recognized that the classical no-slip boundary condition does not always apply, the amplitude of the boundary slip of simple liquids on solid surfaces, and its variation with interfacial properties and flow parameters, is actually a matter of active debate.

Boundary slip effects are usually described in terms of a slip length b relating the interfacial slip velocity V_s, the liquid viscosity η, and the tangential viscous stress σ_{zx} at the solid wall: $V_s = b\sigma_{zx}/\eta = b(\partial V/\partial z)$. The two major characteristics usually considered as determining this slip length are the solid-liquid interactions and the roughness of the solid surface. From a theoretical point of view, it has been shown that simple Lennard-Jones liquids wetting an atomically smooth surface do not slip on it except at very high shear rate when the hydrodynamic boundary condition (HBC) becomes nonlinear [1–3]. Substantial slip develops in nonwetting situations when the contact angle is larger than 90°, with slip lengths reaching 10–50 molecular sizes and depending on the pressure [4]. For a rough surface, two opposite effects have been described: if the liquid wets fully the solid surface, the roughness decreases slip [5], whereas if the liquid wets partially the solid surface, roughness favors the formation of vapor or gas pockets trapped at the solid surface, resulting in large slip length [6–8], and possibly in shear-rate dependent effects [9].

On the experimental side the situation is much less clear. A number of studies involving different techniques report slip effects varying over more than two decades in magnitude, and with qualitatively different shear-rate dependence, for apparently similar systems [10]. Drastically different behaviors are reported for liquids wetting atomically smooth surfaces [11–14], for the influence of surface roughness, [15,16], or for the amplitude and rate dependence of boundary slip on hydrophobic surfaces [17–20]. There is no clear tendency emerging on the role of the interactions or of the roughness, nor is it clearly understood why such large differences are obtained.

Basically two different types of experimental methods have been used to study the HBC of a liquid at a solid wall. Optical methods using tracer particles or molecules to determine the flow field are limited by the resolution of visible optics. Recent methods based on fluorescence techniques allow better resolution [14,21], but they actually measure the transport of tracers close to the wall and the determination of the flow field is indirect. Dissipation methods measure directly the friction induced by the liquid flow and do not suffer intrinsic scale limitation; however, they require one to measure two quantities, a kinematic and a dynamic one. Among those methods, the viscous force induced by a sphere (of radius R) moving orthogonally to a plane has widely been employed, either using a bead glued on an atomic force microscopy (AFM) cantilever [18,20] or a surface force apparatus (SFA) [12,13,17,19]. For one slippery surface, the viscous force induced by the flow at a distance $D \ll R$ is [22]

$$F_v = (6\pi\eta R^2\dot{D}/D)f^*,$$
$$f^* = \frac{1}{4}\left\{1 + \frac{6D}{4b}\left[\left(1 + \frac{D}{4b}\right)\ln\left(1 + \frac{4b}{D}\right) - 1\right]\right\}, \quad (1)$$

with $\dot{D}$ the sphere-plane relative velocity. The factor f^* measuring slip effects varies slowly as a function of the reduced distance D/b, whereas the Reynolds force $6\pi\eta R^2\dot{D}/D$ varies widely with the gap D. As a result, it is necessary for a good determination of the slip length to have accurate measurements of the hydrodynamic force and of the gap D on a significant range of gap values—typically D/b varying up to 20.

In AFM and usual SFA methods, both the hydrodynamic force and the sphere-plane distance are deduced from a single subnanometer resolved distance measurement. The other quantity (the distance in AFM and the force in SFA) is deduced from the calibration of a piezoelectric element,

which raises specific difficulties in evaluating unwanted elastic deformation as well as calibrating the device dynamic response. We present here experiments performed on a dynamic surface force apparatus (DSFA) specifically designed to investigate the hydrodynamics of confined liquids and equipped with two independent subnanometer and time-resolved sensors. Our device measures the oscillating force $F(\omega)$ acting on a plane in response to a small oscillation of a sphere in the direction normal to the plane at frequency $\omega/2\pi$ [23]. The displacement of the plane with respect to a rigid frame is measured by a Nomarski interferometer with a bandwidth of 1 kHz and a quasistatic (steady-state) resolution of 1 Å. With the cantilever spring constant $k = 7200$ N/m used in the experiments reported here, the quasistatic force resolution is 0.7 μN. The relative sphere-plane displacement D is measured by a capacitive sensor whose plates are rigidly mounted on the cantilevers supporting the sphere and the plane, with a bandwidth of 1 kHz and a quasistatic resolution of 1 Å. In dynamic measurements the harmonic components of these two displacements at the frequency $\omega/2\pi$ are measured in amplitude and phase by two double lock-in amplifiers.

Taking into account the noise level of the environment, resolutions, respectively, of 40 nN/$\sqrt{\text{Hz}}$ for the force and 0.1 Å/$\sqrt{\text{Hz}}$ for the relative displacement are achieved in the frequency range 10–100 Hz.

These two independent force and displacement measurements allow an accurate determination of the complex force response $G(\omega) = F(\omega)/h_o$ when the sphere-plane gap is vibrated with amplitude h_o, without the necessity of calibrating any driving elements. This device allows one to check easily for any unwanted elastic deformation: for a Newtonian liquid and rigid surfaces, the response function should have no real part. The imaginary part is the viscous damping due to the flow and can be directly compared to the theoretical expression: $\text{Im}[G(\omega)] = G''(\omega) = 6\pi\eta\omega R^2 f^*/D$ for determining the HBC at the solid wall. The linearity of the HBC is checked easily by changing the amplitude and/or frequency of the excitation at a given value of the gap D.

We use this DSFA to investigate the hydrodynamics of two simple liquids (water and dodecane) confined between symmetric smooth hydrophilic surfaces (plain Pyrex) and asymmetric hydrophilic/hydrophobic surfaces [a plain Pyrex sphere and an octadecyltrichlorosilane (OTS)-coated Pyrex plane]. The choice of an asymmetric system was made to avoid a drying transition by capillary evaporation when the surfaces are close to each other [24]. The surfaces are prepared from commercial float Pyrex by passing them through a flame, washing them in an ultrasonic bath with detergent and distilled water, and rinsing them with purified propanol. The peak-to-peak roughness measured by atomic force microscopy is 1 nm over a 10 μm $\times$ 10 μm area. The OTS-silanized planes are obtained by immersing the surfaces prepared as above in a mixture of 100 μl of OTS and 60 ml of toluene for about 2 h. The AFM topography of the surface prepared with this procedure is very similar to the one of plain Pyrex. The n-dodecane used in the experiments is purchased from Aldrich and is used as obtained. We use ultrapure water (Millipore, MilliQ, 18.2 MΩ cm). Both liquids wet the plain Pyrex surfaces. The contact angle of water on the silanized surfaces measured by the sessile drop method is 105°. The contact angle hysteresis is less than 2°. The surfaces are mounted on the DSFA and dipped in a beaker containing the investigated liquid. All experiments are performed in a clean and thermally isolated room.

Figure 1 shows the inverse of the damping G''^{-1} as a function of the sphere-plane gap D, obtained for dodecane confined between plain Pyrex surfaces. This damping does not depend on the amplitude and increases linearly with the frequency of the oscillatory motion of the sphere in the range investigated, which corresponds to a maximum shear rate of approximately 5×10^3 s^{-1}. The plot is a straight line going through the origin, which corresponds to the well-known Reynolds force valid with a no-slip boundary condition. The slope of this straight line gives an experimental determination of the product ηR^2. From the value of the sphere radius $R = 2.8 \pm 0.1$ mm, we derive a viscosity $\eta = 1.34 \pm 0.07$ mPa s, to be compared to the bulk viscosity of dodecane $\eta_{\text{bulk}} = 1.29$ mPa s at $T = 27$ °C. Confinement has thus no measurable effect on the viscosity of dodecane up to gap values of 4 nm. This plot also shows that the no-slip boundary condition holds within a resolution of 3 nm. The largest source of error here is the determination of the origin, i.e., the position where the sphere and the plane just come into contact. The latter is obtained from the quasistatic interaction force between the surfaces with an error bar of about 2 nm.

Two points must be emphasized in this determination of the HBC. First, the effect of an error in determining the

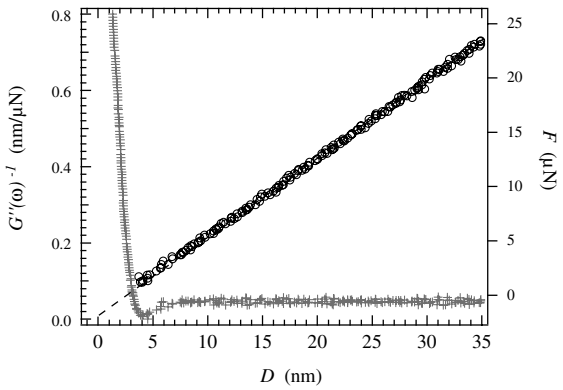

FIG. 1. (○) Inverse of the damping G''^{-1} as a function of the sphere-plane gap D, obtained for dodecane confined between plain Pyrex surfaces and an excitation at a frequency of 39 Hz. (+) Evolution of the quasistatic interaction force as a function of D. The dashed line is a linear extrapolation of the inverse of the damping and shows a no-slip boundary condition within a resolution of 3 nm. Similar damping is obtained with dodecane on an OTS-coated surface.

origin is a mere translation of the G''^{-1} vs D plot along the x axis, but this plot remains a straight line. In the presence of a partial slip boundary condition, G''^{-1} varies as $D/f^*(b/D)$ and this plot would be curved as shown in Fig. 2. Therefore, independently of the determination of the origin, one can estimate a higher bound for a partial slip length only from the shape of a G''^{-1} vs $D - D_{\text{off}}$ curve with D_{off} an arbitrary offset. This higher bound is less than 10 nm. Second, the determination of the HBC does not depend on any preestimated values of the liquid properties (viscosity, diffusivity of optical tracers) or of the geometry of the solid surfaces, unlike data analysis used in AFM experiments or fluorescence measurements.

The damping obtained with dodecane confined between a plain Pyrex sphere and an OTS-coated plane is similar as the one plotted in Fig. 1: no slip is observed within 3 nm resolution.

Figure 2 shows the inverse of the damping obtained with water confined between plain Pyrex hydrophilic surfaces and between the asymmetric system plain Pyrex sphere/OTS-coated plane. A no-slip boundary condition is obtained in the hydrophilic system. From the slope of the plot, we derive the viscosity of the confined water: $\eta = 0.83 \pm 0.06$ mPa s, in good agreement with the viscosity of water at 27 °C: 0.85 mPa s. Here too the viscosity of water does not differ from its bulk value up to confinements of 10 nm. This is in agreement with results of Raviv *et al.* for water confined between mica surfaces [25]. In the asymmetric system, the variation of G''^{-1} with the gap D shows that substantial slip develops at the wall. Since no slip is observed in the hydrophilic system, the only slipping surface is the OTS-coated plane, and we compare the data with the theoretical expression (1). The agreement is very good with a value of the slipping length $b = 19 \pm 2$ nm. This single value of the slip length accounts for the damping observed at all gap values extending from some nanometers up to several hundreds of nanometers. The slip length does not depend on the amplitude or frequency of the sphere motion, showing that the HBC is linear in shear rate. We emphasize that here too the value of the slip length found does not depend on any preestimated value of the liquid or surface properties.

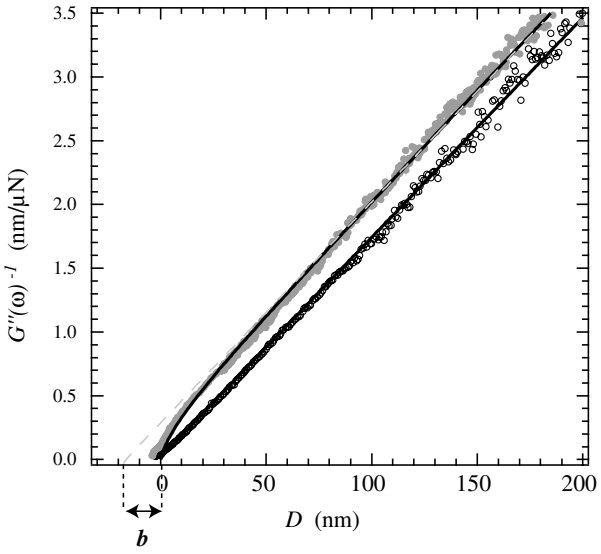

FIG. 2. Inverse of the damping G''^{-1} as a function of the gap D, obtained for water confined between plain Pyrex hydrophilic surfaces (open black circles) and between the asymmetric system plain Pyrex/OTS-coated Pyrex (solid gray circles). The lines correspond to the theoretical expressions for a no-slip boundary condition or a slip length $b = 19$ nm. The dashed line corresponds to the linear extrapolation of the signal in the case of slip; it intersects the D axis at a distance $b = 19$ nm from the origin.

To summarize, our results in perfect and partial wetting configurations do not show any slip effects. This result is in agreement with most data in the literature, some of them obtained with atomically smooth surfaces [11–13] and others with low roughness silica or glass surfaces [20,26]. However, other data report significant slip at a wetting solid-liquid interface [14,27]. We have no explanation for the origin of these discrepancies.

In the nonwetting situation, i.e., with water flowing on a smooth hydrophobic surface, we find a significant slip effect. A single slip length describes the flow dissipation for various values of gap and shear rate. The magnitude of the boundary slip is in good agreement with numerical simulations of interfacial hydrodynamics on nonwetting smooth surfaces [4] as well as with some data in the literature [20,28]. It is, however, much lower than other slip effects reported on hydrophobic or nonwetting systems [10,17,29]. We attribute our moderate slip to the absence of gas trapped at the liquid-solid interface, due to the low roughness and the absence of contamination of the surfaces investigated. We thus think that our result is an *intrinsic* value for the slip of water on smooth hydrophobic surfaces, in the sense that it represents the boundary condition on a small area (tens of μm^2) of surface of roughness less than 1 nm, without effects of contamination or of gas pockets or gas films trapped at the interface.

We compare in more detail our results to the one of Zhu *et al.* [17] obtained with a similar experimental technique (dynamic SFA) on hydrophobic OTE-coated mica surfaces of similar wetting properties to ours. On these substrates Zhu *et al.* report a nonlinear HBC with slip effects increasing with the shear rate above a critical threshold. As stated above, our HBC does not exhibit any nonlinearity with the shear rate. One may conclude that our results represent the low-shear linear limit for the HBC. However, the shear rate may not be the only relevant parameter; absolute pressure is important in all physical mechanisms involving nanobubbles or vapor films at the interface. The maximum amplitude of the oscillating pressure in a SFA flow geometry estimated with a no-slip HBC condition is $P_{\max} = 3\eta R\dot{D}/D^2$. This value does not exceed 10^4 Pa in our experimental conditions, therefore the absolute pressure is always much larger than the water vapor pressure. In [17] the surface radii are larger, which enhances the amplitude of the oscillating pressure and may

facilitate cavitation effects. Another important point is that our results do not meet the low-shear results of Zhu *et al.*, who do no find any slip in this limit. In this low amplitude regime the oscillating pressure should not play any role and both results are linear. However, Zhu *et al.* show in a subsequent paper that the presence of surface roughness reduces slip effects [16]. A possible reason why they do not find slip on hydrophobic surfaces at low shear rate is that the surfaces in [16,17] are densely contaminated by platinum nanoparticles, as they subsequently report [30]. The effect of such contamination on the boundary flow should depend on the driving rate. In the linear regime, surface roughness is expected to decrease slip effects compared to a smooth surface of same wettability. At higher rates, contamination may facilitate nanobubbles cavitation and lower the onset of a nonlinear regime. As discussed in the literature [31], the presence of platinum contamination on mica surfaces depends on their preparation. Other mica-surface experiments to which we compare our findings [11–13] are likely to be contaminant free.

We end with a comment about the very large slip lengths of water on hydrophobic surfaces reported in the literature. In our previous investigation of water flow on OTS-coated Pyrex [10], we found slip effects much larger than here, but with poor reproducibility and poor agreement with the damping expected for a single well-defined slip length. Similar behavior has been reported by Tretheway *et al.* in particle image velocimetry investigation of water flow in OTS-coated glass capillaries [29]. They have evidenced slip effects of large amplitude—200 to 900 nm—variable in space and time, with a velocity profile at the wall significantly different from the parabolic solution of Stoke's equation. These features are coherent with our previous observation in SFA experiments. We believe that they are related to the contamination of the solid wall by nanometric hydrophobic particles. Those particles undergo strong attractive interaction with the hydrophobic wall in water, stick there, and act as nucleation sites for vapor bubbles. Tretheway *et al.* bring direct evidence of this mechanism by running their experiment under an hydrostatic overpressure, for which slip effects disappear within their experimental resolution. In our experiment, changing the environment of the SFA for a clean room changed drastically the results in the hydrophobic case only, while the topographic AFM image of the surfaces remained unchanged, and allowed us to obtain reproducible well-defined slip length of moderate amplitude.

We thank P. Richetti, C. Meinhart, L. Léger, and J. L. Barrat for helpful discussions. We gratefully acknowledge support from the program on microfluidics of the CNRS.

*Electronic address: elisabeth.charlaix@lpmcn.univ-lyon1.fr

[1] P. A. Thompson and M. O. Robbins, Phys. Rev. A **41**, 6830 (1990).
[2] J.-L. Barrat and L. Bocquet, Phys. Rev. E **49**, 3079 (1994).
[3] P. Thompson and S. Troian, Nature (London) **389**, 360 (1997).
[4] J.-L. Barrat and L. Bocquet, Phys. Rev. Lett. **82**, 4671 (1999).
[5] S. Richardson, J. Fluid Mech. **59**, 707 (1973).
[6] P. de Gennes, Langmuir **18**, 3413 (2002).
[7] D. Quéré, Nat. Mater. **1**, 14 (2002).
[8] C. Cottin-Bizonne, J.-L. Barrat, L. Bocquet, and E. Charlaix, Nat. Mater. **2**, 237 (2003).
[9] E. Lauga and M. P. Brenner, Phys. Rev. E **70**, 026311 (2004).
[10] C. Cottin-Bizonne, S. Jurine, J. Baudry, J. Crassous, F. Restagno, and E. Charlaix, Eur. Phys. J. E **9**, 47 (2002).
[11] T. Becker and F. Mugele, Phys. Rev. Lett. **91**, 166104 (2003).
[12] D. Chan and R. Horn, J. Chem. Phys. **83**, 5311 (1985).
[13] J. Israelachvili, J. Colloid Interface Sci. **110**, 263 (1986).
[14] R. Pit, H. Hervet, and L. Léger, Phys. Rev. Lett. **85**, 980 (2000).
[15] E. Bonaccurso, H.-J. Butt, and V. S. J. Craig, Phys. Rev. Lett. **90**, 144501 (2003).
[16] Y. Zhu and S. Granick, Phys. Rev. Lett. **88**, 106102 (2002).
[17] Y. Zhu and S. Granick, Phys. Rev. Lett. **87**, 096105 (2001).
[18] V. S. J. Craig, C. Neto, and D. R. M. Williams, Phys. Rev. Lett. **87**, 054504 (2001).
[19] J. Baudry, E. Charlaix, A. Tonck, and D. Mazuyer, Langmuir **17**, 5232 (2001).
[20] O. I. Vinogradova and G. Yabukov, Langmuir **19**, 1227 (2003).
[21] D. Lumma, A. Best, A. Gansen, F. Feuillebois, J. O. Radler, and O. I. Vinogradova, Phys. Rev. E **67**, 056313 (2003).
[22] O. I. Vinogradova, Langmuir **11**, 2213 (1995).
[23] F. Restagno, J. Crassous, E. Charlaix, M. Monchanin, and C. Cottin-Bizonne, Rev. Sci. Instrum. **73**, 2292 (2001).
[24] H. K. Christenson and P. Claesson, Adv. Colloid Interface Sci. **91**, 391 (2001).
[25] U. Raviv, P. Laurat, and J. Klein, Nature (London) **413**, 51 (2001); U. Raviv, S. Perkin, P. Laurat, and J. Klein, Langmuir **20**, 5322 (2004).
[26] J.-M. Georges, S. Milliot, J. Loubet, and A. Tonck, J. Chem. Phys. **98**, 7345 (1993).
[27] G. Sun, E. Bonaccurso, V. Franz, and H.-J. Butt, J. Chem. Phys. **117**, 10 311 (2002).
[28] C.-H. Choi, K. Johan, K. Westin, and K. Breuer, Phys. Fluids **15**, 2897 (2003).
[29] D. Tretheway and C. Meinhart, Phys. Fluids **14**, L9 (2002); **16**, 1509 (2004).
[30] Z. Lin and S. Granick, Langmuir **19**, 7061 (2003).
[31] J. K. Israelachvili, N. A. Alcantar, N. Maeda, T. E. Mates, and M. Ruths, Langmuir **20**, 3616 (2004).